LA-UR-80-2674

TITLE: CALCULATIONAL METHODS USED TO OBTAIN EVALUATED DATA ABOVE 3 MeV

AUTHOR(S): E. D. Arthur

MASTER

SUBMITTED TO: Workshop on Evaluation Methods and Procedures
Brookhaven National Laboratory
September 22-25, 1980

los alamos
scientific laboratory
of the University of California
LOS ALAMOS, NEW MEXICO 87545

Form No. 836
St. No. 2629
1/79

UNITED STATES
ENERGY RESEARCH AND
DEVELOPMENT ADMINISTRATION
CONTRACT W-7405-ENG-36

CALCULATIONAL METHODS USED TO OBTAIN EVALUATED DATA ABOVE 3 MeV

Edward D. Arthur

Los Alamos Scientific Laboratory, University of California
Theoretical Division
Los Alamos, New Mexico 87545

ABSTRACT

Calculational methods used to provide evaluated neutron data for nuclei between A = 19 and 220 at incident energies above several MeV range from empirical techniques based on cross-section systematics to sophisticated nuclear-model codes that describe the major mechanisms governing neutron reactions in this mass and energy range. Examples of empirical approaches are given along with discussion concerning regions of applicability and accuracies that can be expected. The application of more sophisticated nuclear models (Hauser-Feshbach statistical, preequilibrium, and direct-reaction theories) is discussed, particularly with regard to improved parameter determinations that can be used in such calculations. Efforts to improve the consistency and to unify these theoretical approaches are addressed along with benefits to evaluated data that can be realized through careful application of such nuclear-model techniques.

INTRODUCTION

Evaluated neutron data libraries often rely on calculational techniques to provide necessary cross section, spectral, or angular distribution information. Such instances may involve the need to supplement measured results; to provide data for energy ranges or reaction types lacking experimental data; and, in the most extreme case, to provide data for a nucleus (such as an unstable fission product) where no measurements exist or will likely exist. For medium and heavy nuclei (defined as $19 \leq A \leq 220$ for the purpose of this paper), these techniques range from empirical representations of the systematic behavior of experimental data to more basic approaches employing the Hauser-Feshbach

statistical, preequilibrium, and direct-reaction theories supplemented by use of the spherical or deformed optical model.

In the following sections these techniques are reviewed and their validity examined over the neutron energy range between 3 and 20 MeV. In addition, because of interest in higher energy data motivated by d + Li radiation damage sources, the extension of these techniques up to neutron energies of 50 MeV will be discussed briefly. Because of the wide range in mass and energy covered by this paper, detailed discussions are not feasible; instead examples are provided to illustrate general methods and techniques or to illustrate problem areas. For more detailed discussions, the reader is referred to reviews by Frehaut, [1] Cindro, [2] Qaim, [3] Young et al., [4] and Gardner, [5] as well as the proceedings from various symposiums [6-8] dealing with nuclear theory for applications.

PHENOMENOLOGICAL METHODS BASED ON SYSTEMATIC DATA TRENDS

Interactions of fast neutrons with nuclei in this mass region occur chiefly through elastic and inelastic scattering along with reactions involving the emission of one or more nucleons. Among this latter cross-section type, the (n,2n), (n,p), and (n,α) reactions have been extensively studied over a wide range in mass, albeit restricted to the energy region around 14-15 MeV. From these measurements, parameterizations of cross-section trends as a function of mass or more often as a function of neutron excess, (N-Z)/A, have been developed. Expressions for (n,2n) cross sections have been determined by Lu and Fink [9] that predict such data to within 20% around 14 MeV, while equivalent expressions [10] for (n,p) and (n,α) cross sections exist also having accuracies in the 20-30% range. Recently, Qaim [11-13] and his coworkers have improved such systematics through use of more reliable techniques such as Ge(Li) detectors and isotopically pure samples. Similar efforts [3] have led to systematic studies of the behavior of (n,t), (n,^{3}He), (n,np), and (n,nα) cross sections as a function of mass in the 14-MeV energy range. For the latter two reaction types, the relative paucity of measurements prevent cross-section prediction to better than a factor of two.

Such systematic behavior of cross-section trends are often used in neutron data evaluation, particularly in the absence of experimental data for the given nucleus of interest. In the Livermore ENDL evaluated data library [14] the expressions of Lu and Fink, [9] Gardner and Rosenblum, [15] and Gardner and Yu [16] are often used to provide information covering the 14-MeV values of (n,2n), (n,p), and (n,α) cross sections, respectively. Where such 14-MeV systematics are used, there occurs the difficulty of extending cross-section information to other incident energies. For example, in the Lawrence Livermore Laboratory (LLL) ENDL library, the (n,2n) excitation function is constructed as follows.

From threshold the cross section rises in a sigmoid shape until it reaches a plateau value generally defined (for medium and heavy weight nuclei) by the Lu and Fink formula. Competition from the (n,3n) reaction causes the (n,2n) cross section to smoothly decrease with the maximum (n,3n) cross-section set equal to 60% of the maximum (n,2n) cross-section value. Recent measurements [17-19] of the (n,2n) excitation function from threshold up to 28 MeV provide the opportunity to test this parameterization. In Fig. 1 the ratio of calculated to experimental cross sections for nuclei between ^{89}Y and ^{209}Bi are presented for three ranges of the energy U_R, which is defined as the difference between the incident neutron energy and the (n,2n) threshold. The first region, U_R = 2 MeV, lies fairly close to the (n,2n) threshold; the second, U_R = 6 MeV, occurs for these nuclei in the 14-15 MeV incident energy range; and the third region lies above the (n,2n) plateau region where competition from (n,3n) reactions occur. As to be expected, the agreement is best around U_R = 6 MeV, corresponding to energies for which systematics have been most thoroughly developed. Above and below this energy region, the agreement worsens with a systematic underprediction of 30-40% in the calculated cross section.

Other efforts to parameterize the shape of such cross-section curves appear to be sparse although there have been attempts by Krivan and Munzel [20,21] regarding shapes for (n,p), (n,α), and (n,2n) excitation functions. To do so, the position and value of the maximum cross sections, the half width, and an asymmetry parameter were determined as a function of mass. Such systematics appear to work reasonably well for (n,2n) reactions, but for (n,p) and (n,α) cross sections, there are significant deviations from experimental data.

Empirical parameterizations of 14-MeV cross sections have been supplemented by the use of evaporation theory to provide information concerning cross-section shapes. The foremost example of such a technique is the THRESH code developed by Pearlstein [22] which has been used in almost 50% of the current evaluations in the ENDF library [23] to provide information (either relative shapes or absolute cross sections) for one or more reaction types. As an example, the (n,2n) cross section is calculated from the expression

$$\sigma_{n,2n}(E) = \sigma_{ne} \frac{\sigma_{n,M}}{\sigma_{ne}} \frac{\sigma_{n,2n}(E)}{\sigma_{n,M}} \qquad (1)$$

where σ_{ne} is the nonelastic cross section, and the second factor represents the portion of the nonelastic cross section resulting in neutron emission that is parameterized as a function of the neutron excess, (N-Z)/A. The third factor is calculated from evaporation model theory [24]

$$\frac{\sigma_{n2n}(E)}{\sigma_{n,M}} = \frac{\int_0^{E-B_n} \varepsilon\sigma_c(E)e^{\sqrt{4a(E-\varepsilon)}}d\varepsilon}{\int_0^{E} \varepsilon\sigma_c(E)e^{\sqrt{4a(E-\varepsilon)}}d\varepsilon} \quad , \tag{2}$$

where E, B_n, and ε are the excitation energy of the compound system, the neutron binding energy, and the exit energy of the neutron, respectively; a is the level density parameter; and σ_c is the compound nucleus formation cross section.

The advantages of such a technique as embodied in the THRESH code are its simplicity, (Z and A are the only required input parameters although others may be provided); its speed; and, since the model has been fit to experimental data sets, it is possible to obtain errors and their correlations. The range of uncertainties [25] for (n,p), (n,α), and (n,2n) reactions appear in Table I where they are presented as a function of neutron excess.

A common use of THRESH is to normalize (if necessary) to experimental data at 14 MeV and to then use its calculated results to represent a cross-section excitation function in a given evaluation. To test its ability to predict cross-section shapes, a similar analysis has been performed with THRESH results as was done for ENDL systematics in Fig. 1. Again, the (n,2n) reaction was chosen because of the wide mass range in which experimental excitation functions exist; although in this case the range in neutron excess was extended to include lighter nuclei (^{45}Sc). Similarly, three regions of U_R were chosen to represent incident energy regions near threshold, near the energy at which the maximum cross section occurs, and at energies lying above this plateau region. The results are shown in Fig. 2. For U_R = 2 MeV, the calculated cross sections lie 25-50% higher than the data, indicating the possible effects of gamma-ray competition, angular momentum, or population of discrete levels, none of which are included in THRESH. For lighter nuclei [smaller (N-Z)/A values], such effects are generally absent. (Note that some calculated values deviate systematically over the three U_R ranges, indicating a need to renormalize to better fit the experimental data.) For U_R = 6 MeV, there is generally good agreement, particularly for heavier nuclides (within 10%). However, at U_R = 10 MeV, the code consistently underpredicts the (n,2n) cross section with the most likely cause being that preequilibrium effects [important in (n,2n) reactions at these energies] are not included. From Fig. 2 it appears that use of these techniques to provide cross sections on heavier nuclei above 20 MeV should be exercised with a caution if results are desired to better than within a factor of two.

Phenomenological models play roles in data evaluation other than those connected with cross-section needs. For example, evaluated angular distribution information must be provided for continuum neutron emission, a situation that is made difficult because of the paucity of such experimental measurements and because theoretical models are generally not enough developed to

accurately predict such data. Recently Kalbach and Mann [26] have developed a phenomenological model which with four fitted parameters, knowledge of the energy of the outgoing particle, and division of the cross section into multistep-direct and multistep compound parts can reasonably predict angular distributions in a wide mass range and for secondary energies extending to 60 MeV. Figure 3 compares the predictions of this model to data measured on iron by Hermsdorf et al. [27] for 14.6-MeV neutrons. Sums over three regions of secondary energy are presented, the first representing low emission energies governed mainly by compound nuclear processes, the second dominated by multistep direct processes (here approximated by a total preequilibrium emission fraction), and finally a sum over the range of emission energies from 2 to 11 MeV as may be used to describe the gross angular distribution associated with a total emission spectrum. The overall agreement is good, even within the approximation that the total preequilibrium emission cross section was used in place of the multistep direct component. This indicates the usefulness of this phenomenological representation, particularly at higher incident energies where energy-angle correlations become more important.

NUCLEAR MODELS AND THEIR APPLICATION TO DATA EVALUATION

An application of one or more of the theoretical models that describe neutron reactions in this mass and energy region (optical, Hauser-Feshbach statistical, preequilibrium, and direct) has generally been used to provide some portion of evaluated data files. Most often, this has been through use of the optical model to supplement experimental data regarding total, nonelastic, and elastic cross sections as well as angular distributions from elastic scattering. Likewise, the Hauser-Feshbach statistical model has been used to provide similar data for neutron inelastic scattering from discrete levels. Recently, more sophisticated applications have occurred in which simultaneous calculations of cross sections and spectra have been made for a number of reaction types over a wide incident energy range using consistent input parameter sets.

The optical model and the coupled-channel direct reaction theory are discussed in another contribution to this Workshop. Thus, discussion here will concentrate chiefly on the Hauser-Feshbach statistical and preequilibrium models with particular emphasis placed on the parameters that are used with them. The development of improved techniques for parameter determination along with new model codes that handle tertiary (and higher-order) reactions strengthens the role such techniques will play in future data evaluation. These improvements will be discussed along with problems occurring in the use of such models.

The calculation of cross sections for particle or gamma-ray emission through the Hauser-Feshbach statistical model occurs by use of the expression [28]

$$\sigma_{cc'} = \frac{\pi\lambda^2}{(2i+1)(2I+1)} \sum_{J\pi} \frac{\sum_{s\ell} T_c \sum_{s'\ell'} T_{c'}}{T} W_{cc'} \qquad (3)$$

where i and I are the projectile and target spins, respectively. The term $W_{cc'}$ represents width-fluctuation [29] corrections that must be applied at low energies. Since $W_{cc'} \to 1$ at energies above a few MeV, it will not be described here. To evaluate components appearing in this schematic expression one must have information from optical-model calculations regarding transmission coefficients that describe the compound nucleus formation at a given incident energy as well as ones that described particle emission over a wide secondary energy range. Gamma-ray transmission coefficients must be obtained generally through the use of the Weisskopf [30] single particle or Brink-Axel [31] giant dipole resonance models. Discrete level data must generally be provided, and if a continuum of excitation energies is assumed (because of the lack of sufficient discrete level data) then a level density model and its associated parameters must be employed. Thus application of the Hauser-Feshbach model to data evaluation generally requires a complexity of input parameters much greater than other calculational techniques discussed earlier.

Generally for incident neutron energies above 10 MeV, cross section and spectral results from the statistical model must be modified for nonequilibrium effects through use of the preequilibrium model. To calculate preequilibrium emission, the master equation exciton model [32] has been widely used in evaluations, although some applications of the geometry-dependent hybrid model have also occurred. (For more detail concerning the hybrid model, see the review by Blann. [33]) Within the master equation exciton model, a reaction is assumed to proceed through a variety of particle-hole configurations, starting with simple ones and advancing through more complicated ones until equilibrium is achieved. At each stage during the process there occurs some probability for particle emission. To obtain cross sections and spectra with this model, the following coupled equations must be solved.

$$\frac{dP}{dt}(n,t) = P(n-2,t)\lambda_+(n-2,E) + P(n+2,t)\lambda_-(n+2,E)$$

$$- P(n,t)[\lambda_+(n,E) + \lambda_-(n,E) + \sum_b \int W_b(n,\varepsilon)d\varepsilon] \qquad ,(4)$$

put in by hand

where n is the exciton number (n=p+h), the quantities λ_+ and λ_- represent transition rates to produce increasingly (or decreasingly) complex p-h configurations and W_b is the probability to emit at each stage particles of type b having energy ε. To obtain these rate expressions, the square of the average matrix element for the effective two-body interaction $|M|^2$ must be calculated. In the exciton model this is done empirically through assumption of the form

$$|M|^2 = kA^{-3} E^{-1} \quad . \tag{5}$$

The constant k appearing on the above expression has been determined by Kalbach [34] from the analysis of particle-induced reaction data at energies of tens of MeV. Remaining quantities needed to calculate preequilibrium emission are the compound nucleus formation cross section, inverse cross sections at secondary energies ε, and state densities used to represent p-h configurations.

Recently several new codes employing statistical preequilibrium theories have been developed that should greatly aid in data evaluation. A selected number of these along with their characteristics appear in Table II; a more complete overview has been given by Prince in Ref. 35. The STAPRE, [36] TNG, [37] HAUSER, [38] and GNASH [39] codes carry out multistep reaction calculations with full allowance for angular momentum effects along with preequilibrium corrections. Others like MSPQ [40] and ALICE [41] use evaporation theory for the statistical portion of the calculation along with preequilibrium emission based on the exciton and geometry-dependent hybrid models, respectively. The AMALTHEE [42] and PREANG [43] codes both use matrix methods to solve exactly the master equations of the exciton model without artificial division between preequilibrium and equilibrium components.

Optical, Gamma-ray, and Level-Density Parameters

Transmission coefficients used in Hauser Feshbach calculations should produce accurate compound nucleus formation cross sections while also realistically describing particle emission over a spectrum of emission energies. Such conditions lead to considerable constraints on the optical parameters used so that transmission coefficients obtained using global optical parameter sets can be inadequate for the problem or energy range of interest. Recently improvements in optical model parameters have occurred through the use of the "SPRT" technique developed by Lagrange and co-workers [44] and now used extensively in calculations for evaluated data. The technique employs s- and p-wave strengths to supplement total cross section and elastic angular distribution data so that neutron optical parameters that are typically applicable over the energy range from 10 keV to 20 MeV can be determined. Neutron data are often augmented by the

the use of proton data to extend the range over which such parameters are valid. Figure 4 shows an example of this technique in which coupled-channel calculations of the neutron total cross section for ^{197}Au have been made using the parameters of Delaroche. [45] For ^{197}Au, the parameters are valid up to energies around 60 MeV because of the availability and use of higher energy proton data in the parameter determinations.

The applicability of such optical parameter sets can be verified indirectly through Hauser-Feshbach calculations of processes such as (n,2n) reactions on medium and heavy nuclei from threshold up to energies around 15 MeV. Generally the cross section rises rapidly and if gamma-ray competition is determined using gamma-ray strength functions (see next paragraph), then the calculated shape depends heavily on the neutron transmission coefficients. In addition the calculated cross section can be often determined by transitions to discrete levels in the A-1 nucleus so that level density effects are minimal. Figure 5 illustrates such a case for the ^{89}Y(n,2n) reaction where the optical parameters of Lagrange [46] determined by the SPRT Method and used in GNASH calculations [47] produce good agreement with available experimental data. A similar situation exists for the ^{90}Zr(n,2n) reaction near threshold. However, for incident energies up to 15 MeV, greater than 75% of the calculated cross section results from direct transitions to the 9/2+ ground state of ^{89}Zr. This situation allows the behavior of higher order transmission coefficients to be tested through comparison to experimental data.

As mentioned above, the use of gamma-ray strength functions may offer improvements in the calculation of multistep reactions such as (n,2n), particularly around thresholds where gamma-ray competition is important. Gamma-ray strength functions and their systematics have recently been the subject of an extensive investigation by D. G. and M. A. Gardner [48] to which the reader is referred. In many statistical-model calculations, gamma-ray transmission coefficients are normalized to the $2\pi\langle\Gamma_\gamma\rangle/\langle D\rangle$ ratio where $\langle\Gamma_\gamma\rangle$ and $\langle D\rangle$ are the average gamma-ray width and spacing for s-wave resonances. Such techniques pose little problems for stable nuclei where such data are available experimentally. However, for compound systems lacking this data, these quantities must be deduced from their systematic behavior. This can lead to large errors particularly around closed shell regions where there are large variations in resonance spacings. The use of strength functions to determine gamma-ray transmission coefficients should help alleviate this problem since their normalization should vary slowly between nearby nuclei. Figure 6 illustrates this behavior by showing results of ^{85}Rb and ^{87}Rb capture calculations[48] using identical E1 and M1 strength functions (shown at the left) that reproduce experimental capture cross sections differing by a factor of more than 25.

Progress in improvement of level density parameters and representations has lagged behind the advances described above for optical and gamma-ray strength parameters. Most calculations performed for data evaluations use phenomenological models--generally the constant temperature and Fermi-gas expressions due to Gilbert and Cameron [49] or the back-shifted Fermi-gas model developed by Dilg et al. [50] Mention should also be made concerning the use by Jary [51] in (n,2n) calculations of the Ignatuyk [52] expressions that include an excitation energy dependent level-density parameter. Some improvements in the parameters used with such models have occurred recently due to the work of Reffo [53] on spin cut-off parameters and by Cook [54] regarding updated fits to determine the remaining parameters. Even after these parameter improvements, such models are deficient in describing high excitation energy regions or predicting the ratio of positive to negative parity states as a function of excitation energy. From this point of view, model codes would benefit by the implementation of microscopic level densities using methods such as those of Morretto [55] or Grimes. [56]

Applications

In spite of these shortcomings, nuclear models have been applied successfully to many evaluation problems. Complete and consistent calculations of neutron reactions on barium isotopes from 20 keV to 20 MeV have been made by Strohmaier et al. [57] using the STAPRE code listed in Table II. The TNG code has been used by Fu in the evaluation of neutron cross sections for Ca,-Fe, and Pb, [58-60] and most recently by Larson [61] to calculate neutron reactions on ^{23}Na. Mann et al. have used the HAUSER code to calculate cross sections for the ^{54}Fe(n,p) dosimetry reaction [62] and to calculate alpha-particle production from neutron reactions on copper up to 40 MeV. [63] The GNASH multistep statistical code has been used to calculate reaction cross sections on Fe, Co, [64-65] and most recently on Ni isotopes [66] up to energies of 40-50 MeV. An example of such a calculation is shown in Fig. 7 for the ^{58}Ni(n,2n) reaction. Neutron optical parameters were obtained through the SPRT method while proton and alpha optical parameters were verified through calculation and comparison to proton and alpha induced reaction data up to 40 MeV. Data from $^{58,60-62}$Ni capture reactions provided gamma-ray strength function information. These parameters were then used in preequilibrium-statistical calculations along with direct inelastic scattering cross sections obtained from DWBA calculations. The ^{58}Ni(n,2n) cross section constitutes only a small portion of the total reaction cross section, but reasonable agreement is obtained principally because of the input parameter determinations. Previous calculations [18,67] that relied on global input parameter sets have faired poorly, often missing the experimental results by greater than a factor of two.

Nuclear model calculations can be used to correct some inaccuracies that often exist in evaluated data files. One such area is the representation of neutron emission spectra induced by neutrons on the 10-20 MeV range. Deficiencies in evaluated data have been pointed out by Hetrick et al. [68], occurring most often in cases where evaporation formulas using temperatures determined from level-density parameters are employed for such spectra representation. One such example is the evaluated spectra for tungsten isotopes appearing in ENDF/B-V. In Fig. 8, the evaluated ^{184}W spectrum is compared to measurements by Hermsdorf [27] on natural tungsten using 14.6 MeV neutrons. A large discrepancy exists most noticeably in the secondary energy region where preequilibrium emission and direct reaction effects are most important. Such behavior is corroborated by comparison of calculated neutron spectra [69,70] to results from integral measurements such as those from the pulsed sphere program at Livermore (see Fig. 9). Comparisons to such integral data have proven to be a valuable complement to microscopic data in the 14 MeV region. The calculated emission spectrum that will be used in a new evaluation [71] for tungsten isotopes currently under preparation is shown in Fig. 10. Much better agreement is obtained although some underprediction still exists in the upper end of the spectrum. This would possibly be improved if calculated direct reaction cross sections were included in the comparison.

A consistent application of nuclear models could alleviate another problem occurring in evaluated data files. For example, calculational techniques are sometimes used to provide evaluated neutron cross sections but experimental results are used directly to provide evaluated gamma-ray production data. Inconsistencies between these evaluated data types can lead to energy imbalance problems that can be solved through a consistent use of nuclear-model calculations matched to experimental data. Such problems have been addressed by MacFarlane [71] and Young [4] through energy balance tests of various ENDF evaluations. Some results from these studies are presented in Table III for energies in the 2-20 MeV range. A poor rating indicates that significant (up to 10%) violations occur for conservation of total energy.

As evaluated data libraries are extended to higher energies, the demands placed upon model calculations will increase because of the general consensus that experimental measurements cannot satisfy all of the data needs for energies above 20 MeV. In such instances, calculations must be performed in which complicated reaction chains must be followed to include all major neutron and charged-particle producing reactions. Figure 11 shows such a chain that was used for GNASH calculations on iron [64] up to 40 MeV. Calculated cross sections using this chain are shown in Fig. 12, indicating that contributions for reactions such as (n,2np) [sum of (n,npn) + (n,pnn) + (n,2np)] dominate at higher energies over those involving solely neutron emission, again illustrating the need for such detail in the calculation.

Problems that occur in model calculations below 20 MeV are magnified considerab at higher energies, particularly with regard tc level density representations and parameters. This is due in part to the higher excitation energies involved and because nuclei are reached that lie further away from the lines of stability at which most experimental information exists. Such deficiencies can be compensated to some degree through comparison to higher energy charged-particle induced reaction data that can be used to verify and optimize parameters for level density, preequilibrium, and other ingredients needed in such calculations.

Improvements in Nuclear Models

There are several areas of theoretical improvements that will be useful for future data evaluation. One such example is the extension, for preequilibrium emission, of the generalized master equation of Mantzouranis et al. [73] by Gruppelar and Akkerman [74] to the theoretical analysis of angular distributions induced by 14.6 MeV neutrons. Satisfactory results were obtained over a wide mass range (berylium to bismuth) after adjustment of two global parameters.

The unification of preequilibrium and the Hauser-Feshbach statistical model has been pursued by Fu [75] at ORNL through incorporation of angular momentum effects into the preequilibrium model. The result is a form that becomes compatible with standard Hauser-Feshbach techniques when equilibrium is reached. A part of this is achieved through the determination and use of level and state density parameters that are consistent between the two models, a situation that has generally been lacking in the past. This unified model, after determination of two parameters through comparison to 14.6 MeV neutron emision data for iron, has been applied to calculation of the neutron and charged-particle emission spectra on 12 isotopes having recent experimental data. Initial results from such calculations have proven satisfactory as shown in Fig. 13 where comparisons are made to experimental neutron production spectra. This model, in addition to providing cross sections and spectral information, also allows angular distribution information to be obtained for continuum particle emission.

UNCERTAINTIES RESULTING FROM APPLICATION OF CALCULATIONAL TECHNIQUES

Along with the evaluated data that can be obtained using the calculational methods outlined in this paper, there is a need to provide information about uncertainties arising from use of such techniques, especially in areas lacking experimental data. By

use of the empirical techniques discussed at the beginning of this paper, fits can be made to experimental data using a given parameter set, from which uncertainties and their correlations can be ascertained. An example of such results appeared in Table I. However, if a model is extended significantly beyond the region where its parameters and their errors were obtained, then the confidence that can be placed upon calculated results and errors declines considerably.

If nuclear models are used to determine evaluated data where no experimental measurements exist then the error problem becomes increasingly more difficult. In such cases, the number of input parameters is greater and often because of lengthy computational times it is not possible to vary each input parameter to examine the sensitivity of the calculated results to it. Also, for some excitation energy regions or nuclei far removed from stability, the theoretical models used may have little or no validity. There are however cases where meaningful errors and their correlations can be obtained for parameters used in theoretical analyses. One such example is the use of chi-square minimization methods to obtain optical parameters from fits to experimental data. Also, some nuclear-model codes require relatively little computer time, and studies of the sensitivity of calculated results can be made as a function of a significant number of parameters. One such example is the analysis by Pearlstein [76] of neutron emission spectra induced by 14 MeV neutrons over the mass range from sodium to bismuth. The preequilibrium-evaporation code ALICE [41] was used to obtain covariances and correlations for several fitted parameters. The result was a global parameter set that could produce agreement to within 30% of the measured results in over 70% of the cases studied.

The estimation of errors using more complicated Hauser-Feshbach techniques (with preequilibrium corrections) generally is more vague and relies on the systematic behavior of input parameters within some realm of physically acceptable values. The error estimates made in calculations of neutron reactions on barium isotopes by Strohmaier [57] follow this pattern where relatively small estimates (10%) were made for neutron emission cross sections because of well-determined neutron parameters and a good supply of experimental data. For other cases such as charged-particle reactions lacking well-determined input parameters or data, estimated errors were significantly larger (40%).

CONCLUSIONS

Some of the calculational techniques used to provide evaluated data for medium and heavy mass nuclei in the neutron energy range above 3 MeV have been reviewed. Empirical techniques play a role when cross-section estimates are desired based on systematic data trends or in situations where more basic models are not sufficiently developed to produce adequate agreement with

experimental results. However, the improvement in input parameters and the availability of new, sophisticated nuclear model codes have resulted in an increased use of theoretical methods to provide cross sections and spectral information. The extension of evaluated data to higher energies promises further improvement in these theoretical techniques. It should be remembered, however, that underlying these discussions of empirical and theoretical methods is the realization of the importance of having adequate experimental data with which to verify and improve such techniques.

REFERENCES

1. J. Frehaut, "Neutron-Induced Cascade Reactions," in Proc. Int. Conf. on the Interactions of Neutrons with Nuclei, Lowell, MA (1976), p. 336.

2. N. Cindro, "(n,x) Reactions on Medium and Heavy Nuclei," Proc. Int. Conf. on the Interactions of Neutrons with Nuclei, Lowell, MA (1976), p. 348

3. S. M. Qaim, "Recent Advances in the Study of Some Neutron Threshold Reactions," Proc. Int. Conf. on Neutron Physics and Nuclear Data, Harwell (1978), p. 1088.

4. P. G. Young et al., "Application of Nuclear Models," Int. Conf. on Nuclear Cross Sections for Technology, Knoxville, TN (1979).

5. D. G. Gardner, "Recent Developments in Nuclear Reaction Theories and Calculations," in Proc. of Sym. on Neutron Cross Sections from 10-50 MeV, Brookhaven (1980).

6. T. Fuketa, Ed., Proc. of the EANDC Topical Discussion on "Critique of Nuclear Models and Their Validity in the Evaluation of Nuclear Data," NEANDC(J)38L (1975).

7. "Nuclear Theory in Neutron Nuclear Data Evaluation," Vols. 1 and 2, IAEA-190 (1976).

8. A. Salam, Ed., "Nuclear Theory for Applications, Proceedings of a Course," IAEA-SMR-43, Trieste (1978).

9. Wen-deh Lu and R. W. Fink, Phys. Rev. C4, 1173 (1971).

10. V. N. Levkovskii, Sov. J. Nucl. Phys. 18, 361 (1974).

11. S. M. Qaim, Nucl. Phys. A185, 614 (1972).

12. N. I. Molla and S. M. Qaim, Nucl. Phys. A283, 269 (1977).

13. S. M. Qaim, "Nuclear Data Needs for Radiation Damage Studies," in Proc. of Advisory Group Mtg. on Nuclear Data for Fusion Reactor Technology, IAEA-TECDOC-223 (1979).

14. R. J. Howerton et al., "The LLL Evaluated Nuclear Data Library (ENDL)," UCRL 50400, Vol. 15A (1975); M. A. Gardner and R. J. Howerton, "ACTL: Evaluated Neutron Activation Cross-Section Library," UCRL-50400, Vol. 18 (1978).

15. D. G. Gardner and S. Rosenblum, Nucl. Phys. A96, 121 (1967).

16. D. G. Gardner and Y. W. Yu, Nucl. Phys. 60, 49 (1964).

17. J. Frehaut and G. Mosinski, "Measurement of (n,2n) and (n,3n) Cross Sections for Incident Energies between 6 and 15 MeV," in Nuclear Cross Sections and Technology Conference Proceedings NBS-S425, p. 855 (1975).

18. B. P. Bayhurst et al., Phys. Rev. C12, 451 (1975).

19. L. R. Veeser et al., Phys. Rev. C16, 1792 (1977).

20. V. Krivan and H. Munzel, J. Inorg. Nucl. Chem. 34, 2993 (1972).

21. V. Krivan and H. Munzel, J. Inorg. Chem. 34, 2989 (1972).

22. S. Pearlstein, J. Nucl. Energy 27, 81 (1973); S. Pearlstein, "Program THRES2, A Revision of THRESH," Brookhaven National Laboratory report (1975).

23. R. Kinsey, "ENDF/B Summary Documentation, 3rd Edition, (ENDF/B-V)," Brookhaven report BNL-NCS-17541 (1979).

24. J. M. Blatt and V. Weisskopf, Theoretical Nuclear Physics (Wiley, New York, 1952), p. 365.

25. S. Pearlstein, "Neutron Cross Sections and Their Uncertainties Obtained from Nuclear Systematics," in Nuclear Cross Sections and Technology Conference Proceedings NBS-S425, p. 332 (1975).

26. C. Kalbach and F. M. Mann, "Phenomenology of Preequilibrium Angular Distributions," in Proc. Symp. on Neutron Cross Sections from 10-50 MeV, Brookhaven (1980).

27. D. Hermsdorf et al., "Differentielle Neutronenemissionsquerschnitte," ZFK-277, Dresden, DDR (1974).

28. W. Hauser and H. Feshbach, Phys. Rev. 87, 366 (1952).

29. P. A. Moldauer, Phys. Rev. C12, 744 (1975).

30. J. M. Blatt and V. F. Weisskopf, Theoretical Nuclear Physics (John Wiley, New York, 1952), p. 627.

31. D. M. Brink, Thesis, Oxford University (1955), unpublished; P. Axel, Phys. Rev. 126, 671 (1962).

32. C. Kalbach, Acta. Phys. Slov. 25, 100 (1975).

33. M. Blann, Annual Reviews of Nuclear Science 25, 123 (1975).

34. C. Kalbach, Z. Phys. A287, 319 (1978).

35. A. Prince, "Statistical Theory Applications and Associated Computer Codes," p. 231; and "Computer Codes Incorporating Preequilibrium Decay," p. 305, in Proc. of the Course on Nuclear Theory for Applications, IAEA-SMR-43, Trieste (1978).

36. M. Uhl and B. Strohmaier, "STAPRE: A Computer Code for Particle-Induced Activiation Cross Sections," IRK 76/01 (1976).

37. C. Y. Fu, "Development of a Two-Step Hauser-Feshbach Code With Precompound Decays and Gamma-Ray Cascades," Nuclear Cross Sections and Technology Conference Proceedings, NBS-S425, p. 328 (1975).

38. F. M. Mann, "HAUSER-4: A Computer Code to Calculate Nuclear Cross Sections," HEDL-TME-76-80 (1976).

39. P. G. Young and E. D. Arthur, "GNASH: A Preequilibrium-Statistical Nuclear Model Code for Calculation of Cross Sections and Emission Spectra," LA-6947 (1977).

40. J. Jary, "MSPQ: A FORTRAN Code for Cross Section Calculations Using a Statistical Model with Preequilibrium Effects," INDC(FR)10L (1977).

41. M. Blann, "Overlaid ALICE," University of Rochester report COO-3494-29 (1975).

42. O. Bersillon and L. Faugere, "AMALTHEE" A Code for Spectra and Cross Section Calculations within the Exciton Model," NEANDC(D)191L (1977).

43. J. M. Akkermans and H. Gruppelaar, "Calculation of Preequilibrium Angular Distributions with the Exciton Model Code PREANG," ECN-60 (1979).

44. J. P. Delaroche, Ch. Lagrange, and J. Salvy, "The Optical Model with Particular Considerations of the Coupled-Channel Optical Model," IAEA-190, p. 251 (1976).

45. J. P. Delaroche, "Potential Optique Nucleon - ^{197}Au entre 10 keV et 57 MeV," Proc. of the Int. Conf. on Neutron Physics and Nuclear Data, Harwell (1978), p. 366.

46. Ch. Lagrange, "Optical Model Parameterization between 10 keV and 20 MeV - Applicable to the ^{89}Y and ^{93}Nb Spherical Nuclei," in Proc. 3rd National Soviet Conf. on Neutron Physics, Kiev (1975) CONF-75061154 Atomizdat (1976).

47. E. D. Arthur, "Calculations of Neutron Cross Sections on Isotopes of Yttrium and Zirconium," LA-7789-MS (1979).

48. D. G. Gardner et al., "A Study of Gamma-Ray Strength Functions," UCID-18759 (1980).

49. A. Gilbert and A. G. W. Cameron, Can. J. Phys. 43, 1446 (1965).

50. W. Dilg et al., Nucl. Phys. A217, 269 (1973).

51. J. Jary and J. Frehaut, "Level Density Dependence of (n,γ), (n,n'), and (n,2n) Reaction Cross Sections," in Progress Report of the Neutron and Nuclear Physics Division for the Year 1979, CEA-N-2134, p. 185 (1980).

52. A. V. Ignatuyk et al., Sov. J. Nucl. Phys. 21, 255 (1975).

53. G. Reffo, "Parameter Systematics for Statistical Theory Calculations of Neutron Reaction Cross Sections," CNEN-RT/FI-80 (1980).

54. J. L. Cook and E. [illegible]. Rose, "An Evaluation of the Gilbert-Cameron Level Density Parameters," AAEC/E419 (1977).

55. L. G. Morretto, Nucl. Phys. A185, 145 (1972).

56. S. M. Grimes et al., Phys. Rev. C19, 2378 (1979).

57. B. Strohmaier et al., Nucl. Sci. Eng. 65, 368 (1974).

58. C. Y. Fu, Atomic Data and Nucl. Data Tables 17, 127 (1976).

59. C. Y. Fu and F. G. Perey, ENDF/B-V MAT 1326 (1979).

60. C. Y. Fu and F. G. Perey, Atomic Data and Nucl. Data Tables 17, 409 (1975).

61. D. C. Larson, to be published.

62. R. E. Schenter et al., "Evaluation of the $^{58}Fe(n,\gamma)$ and $^{54}Fe(n,p)$ Reactions for the ENDF/B-V Dosimetry File," in Proc. of Int. Conf. on Nuclear Cross Sections for Technology, Knoxville, TN (1979).

63. D. W. Kneff et al., Nucl. Technology 49, 498 (1980).

64. E. D. Arthur and P. G. Young, "Evaluation of Neutron Cross Sections to 40 MeV for $^{54,56}Fe$," in Proc. Symp. on Neutron Cross Sections from 10-50 MeV, Brookhaven (1980).

65. E. D. Arthur et al., "Calculation of ^{59}Co Neutron Cross Sections between 3 and 50 MeV," in Proc. of Symp. on Neutron Cross Sections from 10-50 MeV, Brookhaven (1980).

66. R. C. Harper and E. D. Arthur, to be published.

67. A. Marcinkowski, "Measurements and Evaluation of Fast Neutron Cross Section Data for Reactor Dosimetry," INDC(NDS)103/M (1979).

68. D. M. Hetrick et al., "Status of ENDF/B-V Neutron Emission Spectra Induced by 14 MeV Neutrons," ORNL/TM 6637 (1979).

69. G. P. Estes and R. E. Seamon, "More Integral Testing of ENDF/B-V Data," to be presented at the ANS Winter Meeting (Nov. 1980).

70. R. J. Howerton, "Data Testing Results for the ENDF/B-V Evaluated Neutron Data File," UCID-18731 (1980).

71. E. D. Arthur, C. A. Philis, P. G. Young, and A. B. Smith, to be published.

72. R. E. MacFarlane, Trans. Am. Nuc. Soc. 33, 681 (1979).

73. G. Mauntzouranis et al., Phys. Lett 57B, 220 (1975).

74. H. Gruppelaar and J. M. Akkermans, "Comparison of Experimental and Calculated Neutron Emission Spectra and Angular Distributions," in Proc. Symp. on Neutron Cross Sections from 10-50 MeV, Brookhaven (1980).

75. C. Y. Fu, "A Consistent Nuclear Model for Compound and Precompound Reactions with Conservation of Angular Momentum," ORNL/TM 7042 (1980).

76. S. Pearlstein, Nucl. Sci. and Eng. 68, 55 (1978).

TABLE I

UNCERTAINTY RANGES (%) FOR THRESH CROSS SECTION RESULTS AS A FUNCTION OF NEUTRON EXCESS (Ref 25)

Reaction	Neutron Excess (N-Z)/A			
	0.03-0.05	0.05-0.1	0.1-0.15	0.15-0.2
(n,2n)	20-50	10	10	10
(n,p)	20-25	20-30	20-40	30-150
(n,α)	25	25-40	30-60	40-150

TABLE II

SOME RECENT NUCLEAR MODEL CODES USED FOR EVALUATION PURPOSES

Code	Author	Method	$\frac{d\sigma}{d\varepsilon}$	$\frac{d\sigma_\gamma}{d\varepsilon}$ [a]	$\frac{d\sigma}{d\Omega}$	$\frac{d^2\sigma}{d\varepsilon d\Omega}$	σ_x [b]	σ_f [c]
ALICE	Blann	Evaporation and geometry-dependent hybrid preequilibrium	x					
AMALTHEE	Bersillon & Faugere	Matrix solution of master equations exciton model for $t \to \infty$	x					
GNASH	Young & Arthur	Multistep Hauser-Feshbach, master equations exciton model	x	x			x	x
HAUSER5	Mann	Multistep Hauser-Feshbach, master equations exciton model	x	x	x		x	x
MSPQ	Jary	Evaporation and exciton model preequilibrium	x					x
PREANG	Akkermans, Gruppelaar & Luider	Matrix solution of generalized master equation exciton model	x			x		
STAPRE	Uhl & Strohmaier	Multistep Hauser-Feshbach, master equation exciton model	x	x			x	x
TNG	Fu	Unified multistep Hauser-Feshbach and preequilibrium with angular momentum conservation	x	x	x	x	x	

(a) gamma-ray spectra and cross sections

(b) isomeric state cross sections

(c) fission cross sections

TABLE III

QUALITATIVE RATING OF ENERGY BALANCE FOR ENDF/B-V MATERIALS IN THE ENERGY RANGE 2-20 MeV (Ref. 72)
(G = good, F = fair, P = poor)

^{19}F	F	^{55}Mn	P
^{23}Na	F	Fe	P
Mg	F	^{59}Co	P
^{27}Al	F	Ni	P
Si	G	Cu	*
^{31}P	F	Mo	*
^{32}S	F	^{138}Ba	F
Cl	*	^{181}Ta	P
K	P	^{182}W	P
Ca	G	^{183}W	P
Ti	F	^{184}W	P
V	F	^{186}W	P
Cr	P	Pb	F

*Masked by element effect

FIGURE CAPTIONS

1. The ratio of (n,2n) cross sections calculated using the LLL ENDL empirical methods to experimental results for nuclei ranging from ^{89}Y to ^{209}Bi are presented for three regions of U_R [U_R = incident energy - (n,2n) threshold energy]. These regions correspond to energies slightly above the (n,2n) threshold, to energies where the (n,2n) cross sections reach a maximum, and to energies above the plateau region where (n,3n) competition occurs.

2. The ratio of (n,2n) cross sections calculated using the THRES2 [22] code to data for nuclei ranging from ^{45}Sc to ^{209}Bi. The same U_R regions are used as were defined in Fig. 1.

3. Angular distributions of emitted neutrons from 14.6 MeV neutron interaction with iron calculated using the Kalbach-Mann [26] expressions are compared to the Hermsdorf [27] data for several ranges of secondary energy.

4. The ^{197}Au total cross section determined from coupled-channel calculations using the Delaroche optical parameters [45] are compared to experimental data.

5. Cross sections for the $^{89}Y(n,2n)$ reaction obtained from GNASH calculations using the Lagrange optical parameters [46] are compared to recent measurements [17-19] of this reaction.

6. Calculated $^{85,87}Rb(n,\gamma)$ cross sections [48]. The same E1 strength function (shown at the left) used for both isotopes produces good agreement with experimental results.

7. Cross sections calculated for the $^{58}Ni(n,2n)$ reaction using consistent sets of input parameters are compared to experimental data.

8. The partial and total neutron emission spectra from the ENDF/B-V ^{184}W evaluation are compared to the data of Hermsdorf [27] measured at 14.6 MeV for natural tungsten.

9. Calculated spectra obtained through use of the ENDF/B-V evaluated tungsten data are compared to experimental results from 14-MeV pulsed-sphere measurements.

10. The partial and total neutron emission spectra obtained from new calculations [71] on ^{184}W that include preequilibrium and direct contributions are compared to the Hermsdorf data.

11. The reaction chain used for the calculation of neutron reactions on iron [64] up to energies of 40 MeV.

12. Theoretical n + ^{56}Fe cross sections obtained from GNASH calculations using th reaction chain shown in Fig. 11. Note that above 30 MeV, processes such as (n,np) and (n,2np) compete with and begin to dominate over reactions involving solely neutron emission.

13. Neutron production spectra obtained through calculations using unified Hauser-Feshbach-preequilibrium model of Fu [75] are compared to the 14.6 MeV Hermsdorf data for eight natural elements.

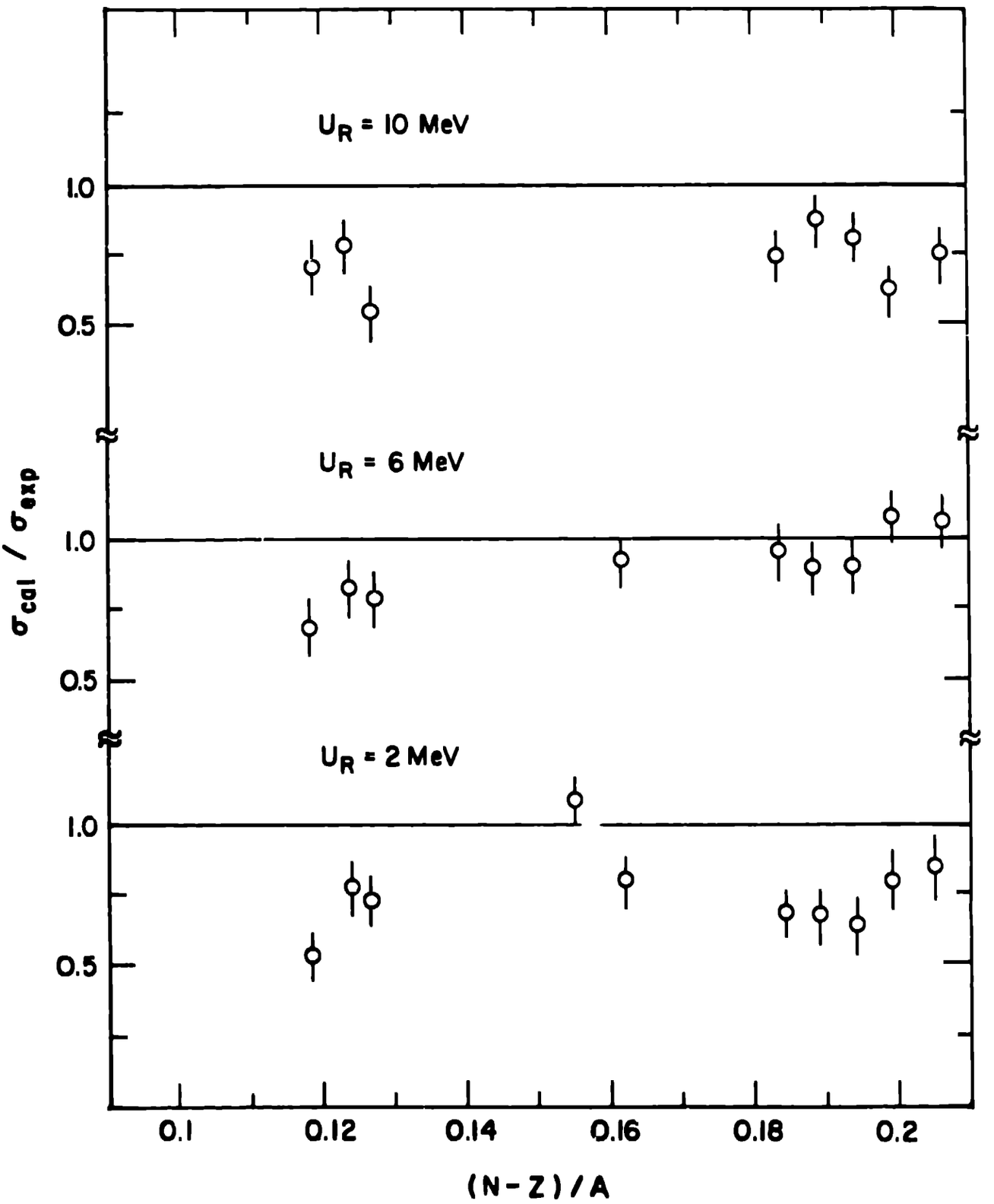
U_R = 10 MeV
U_R = 6 MeV
U_R = 2 MeV
1.0
0.5
1.0
0.5
1.0
0.5
$\sigma_{cal} / \sigma_{exp}$
0.1
0.12
0.14
0.16
0.18
0.2
(N - Z) / A

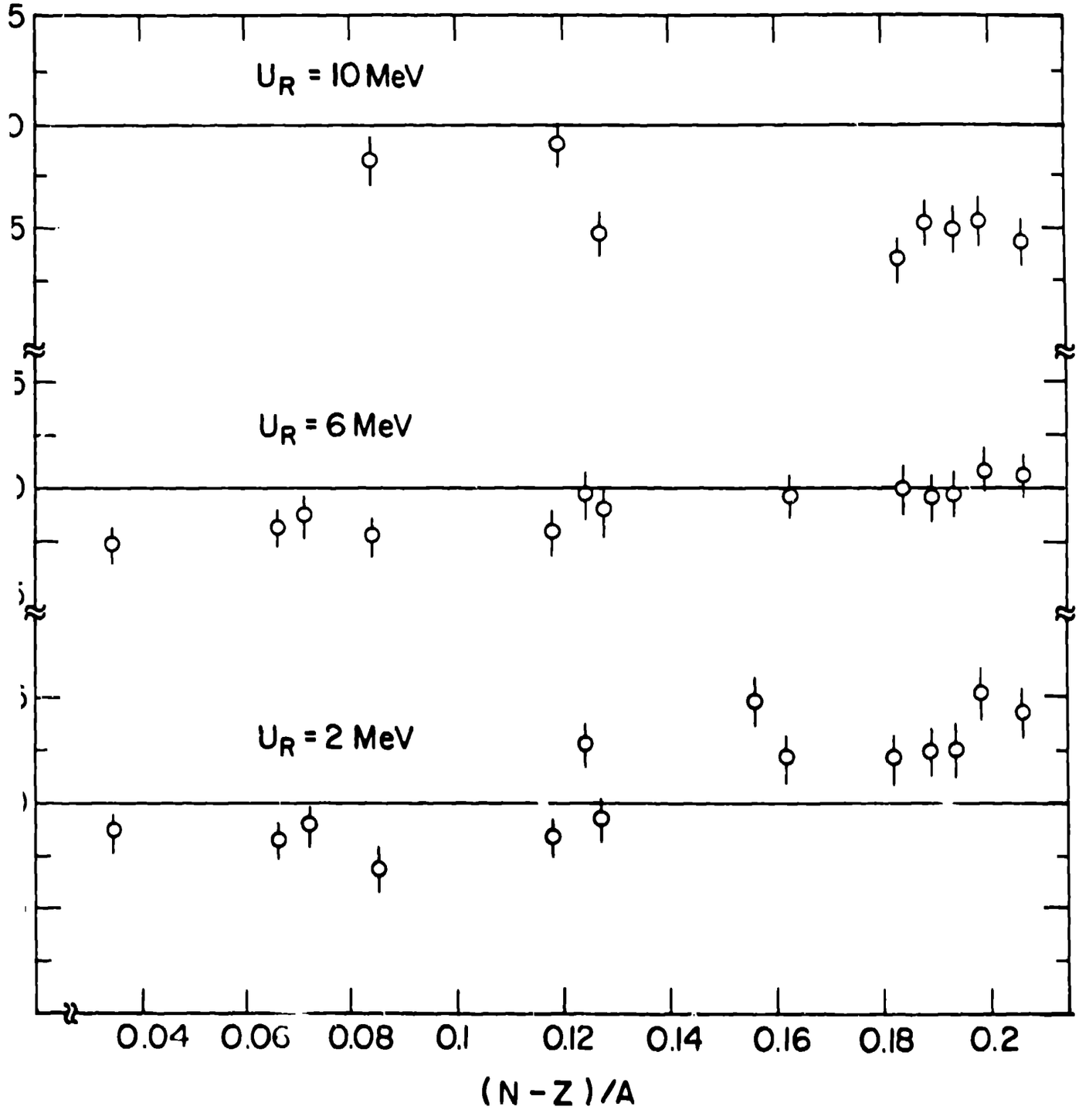
U_R = 10 MeV
U_R = 6 MeV
U_R = 2 MeV
0.04
0.06
0.08
0.1
0.12
0.14
0.16
0.18
0.2
(N - Z) / A

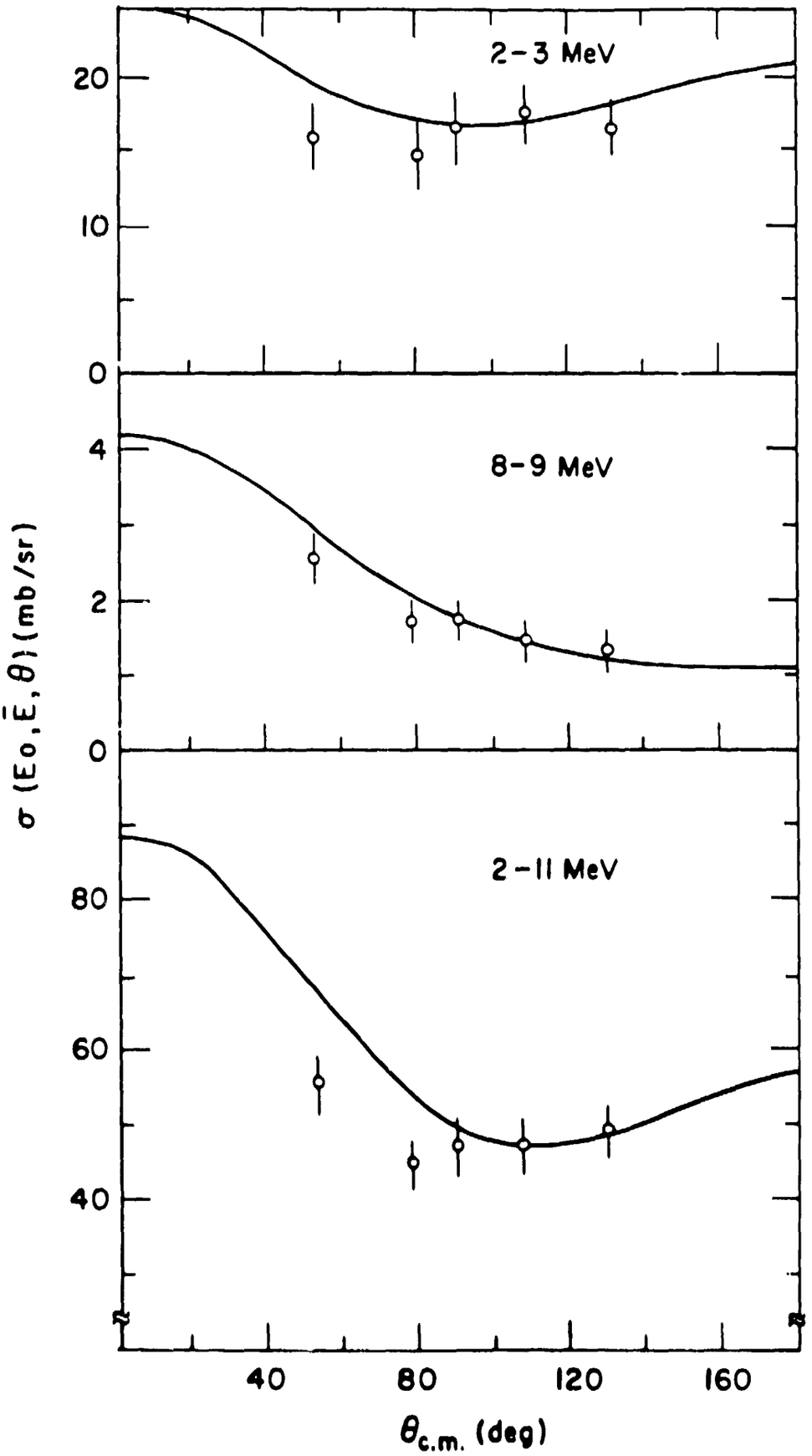
2-3 MeV
8-9 MeV
2-11 MeV
20
10
0
4
2
0
80
60
40
40
80
120
160
σ (Eo, Ē, θ) (mb/sr)
θc.m. (deg)

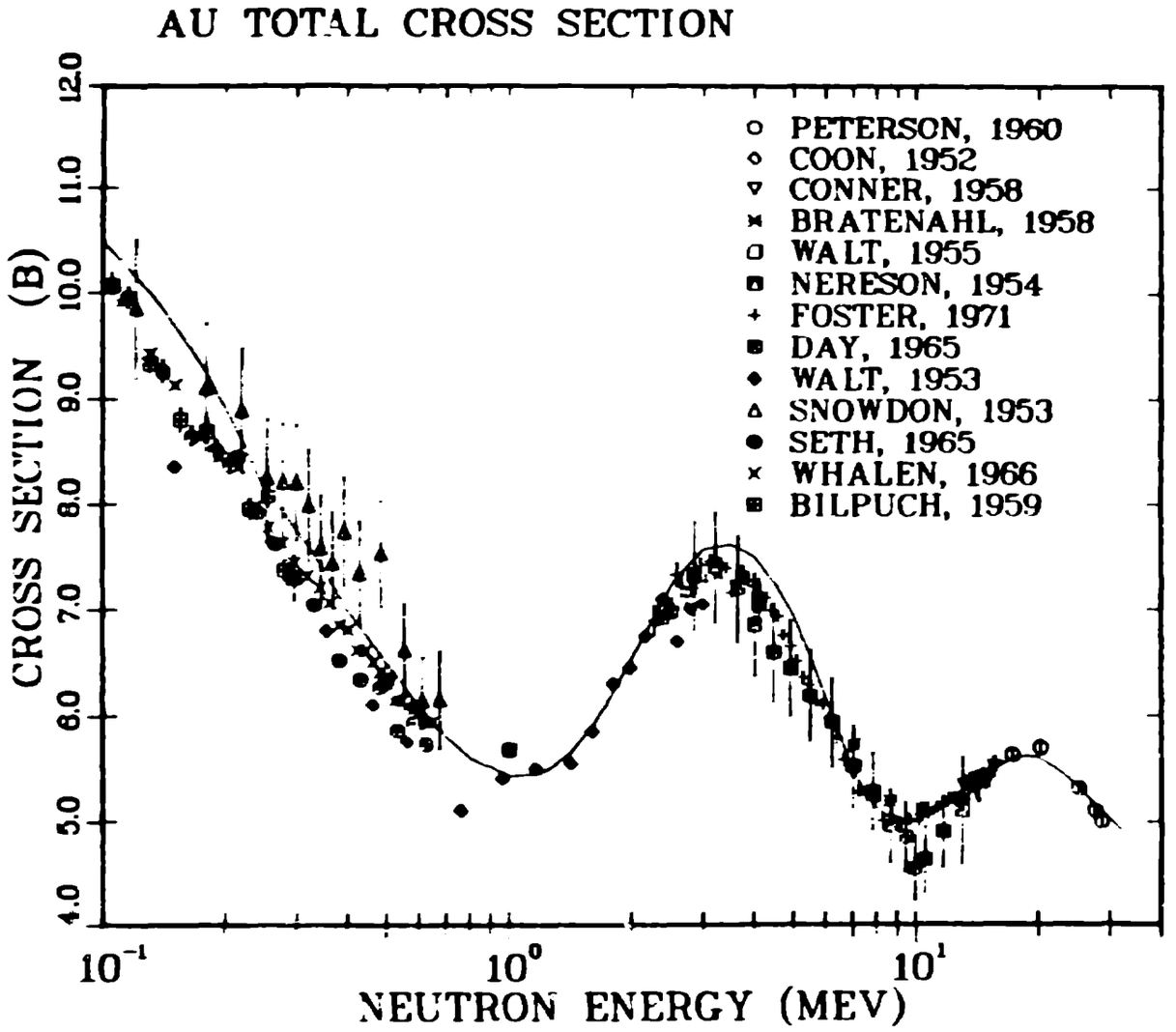
AU TOTAL CROSS SECTION
CROSS SECTION (B)
12.0
11.0
10.0
9.0
8.0
7.0
6.0
5.0
4.0
10^{-1}
10^{0}
10^{1}
NEUTRON ENERGY (MEV)
PETERSON, 1960
COON, 1952
CONNER, 1958
BRATENAHL, 1958
WALT, 1955
NERESON, 1954
FOSTER, 1971
DAY, 1965
WALT, 1953
SNOWDON, 1953
SETH, 1965
WHALEN, 1966
BILPUCH, 1959

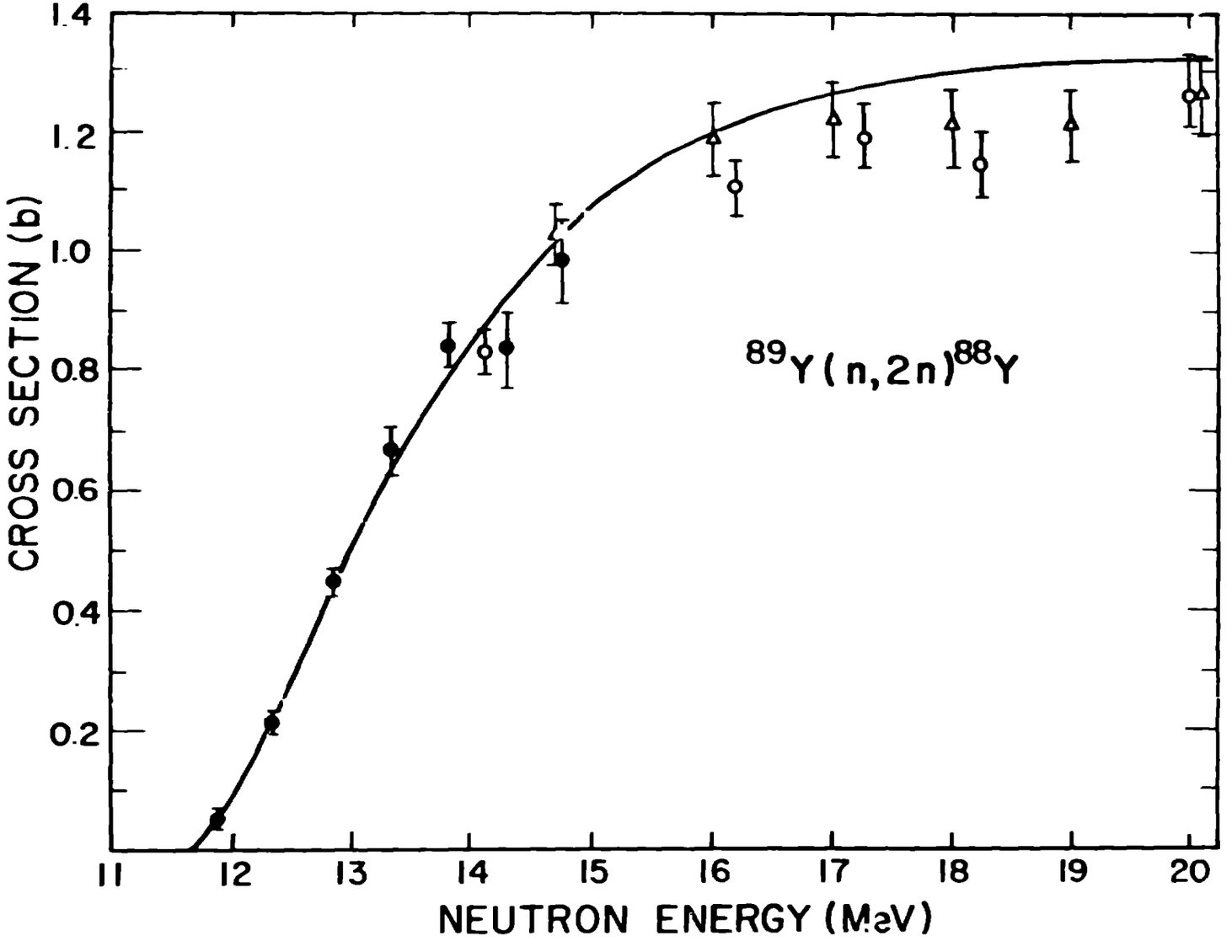
1.4
1.2
1.0
0.8
0.6
0.4
0.2
CROSS SECTION (b)
$^{89}Y(n,2n)^{88}Y$
11
12
13
14
15
16
17
18
19
20
NEUTRON ENERGY (MeV)

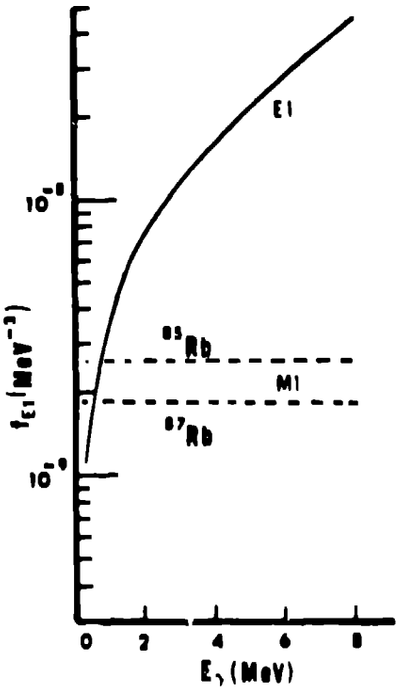
E1
M1
^{85}Rb
^{87}Rb
10^{-8}
10^{-9}
f_{E1} (MeV^{-3})
0
2
4
6
8
E_γ (MeV)

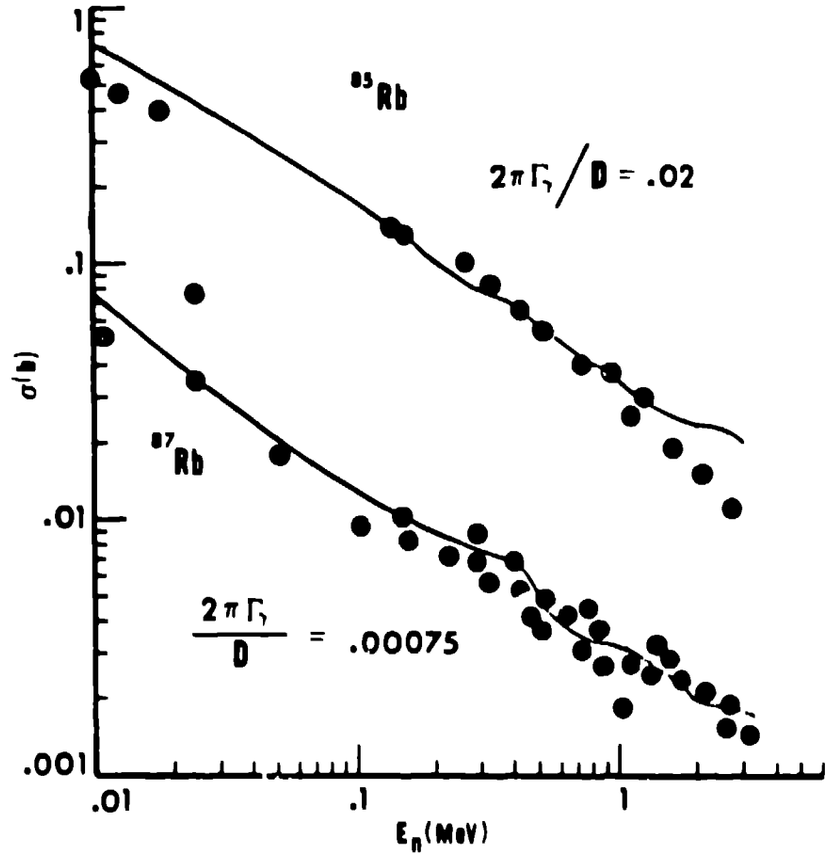
^{85}Rb
$2\pi\Gamma_\gamma/D$ = .02
^{87}Rb
$\frac{2\pi\Gamma_\gamma}{D}$ = .00075
1
.1
.01
.001
σ(b)
.01
.1
1
E_n(MeV)

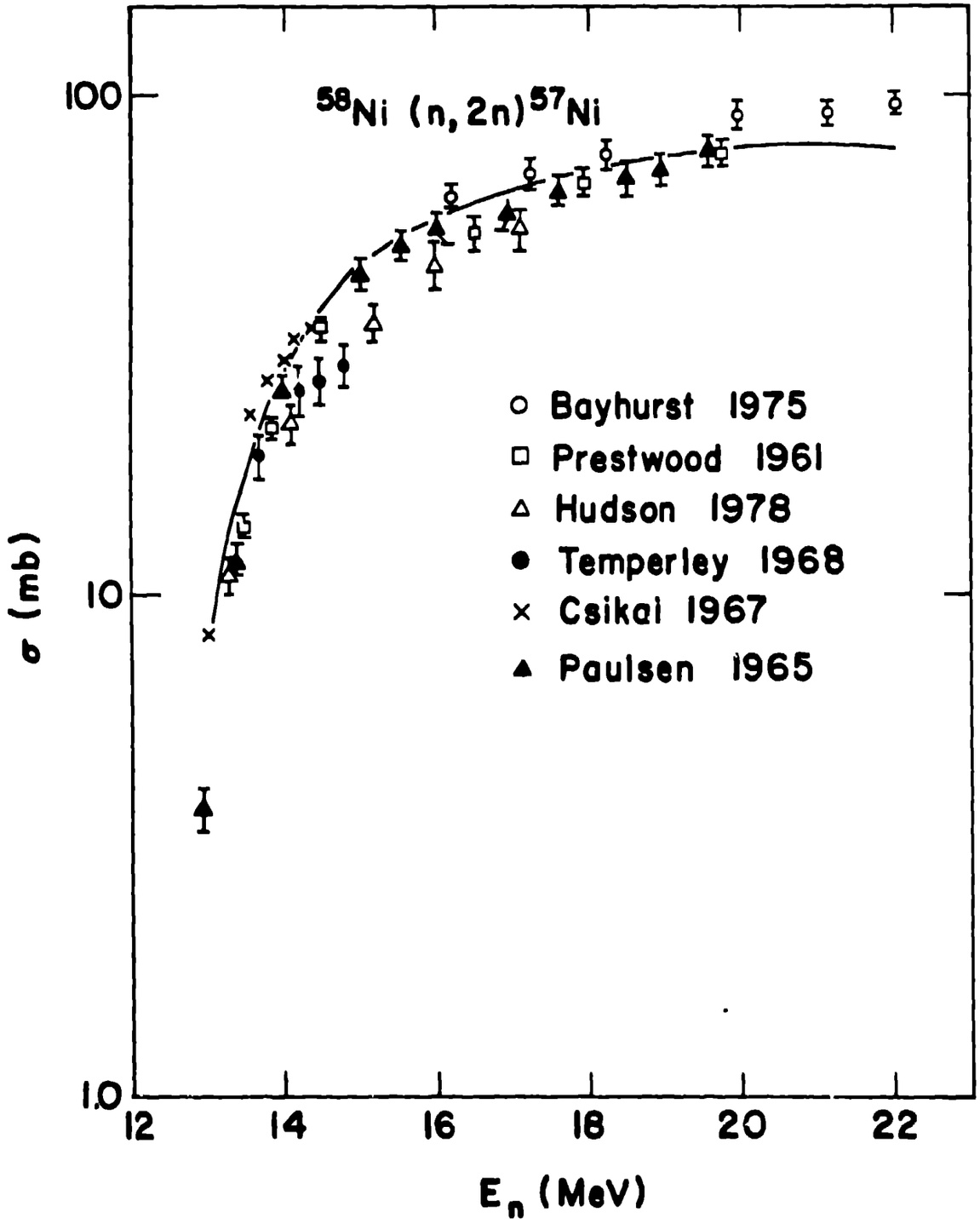
^{58}Ni (n, 2n)^{57}Ni
Bayhurst 1975
Prestwood 1961
Hudson 1978
Temperley 1968
Csikai 1967
Paulsen 1965
σ (mb)
100
10
1.0
12
14
16
18
20
22
E_n (MeV)

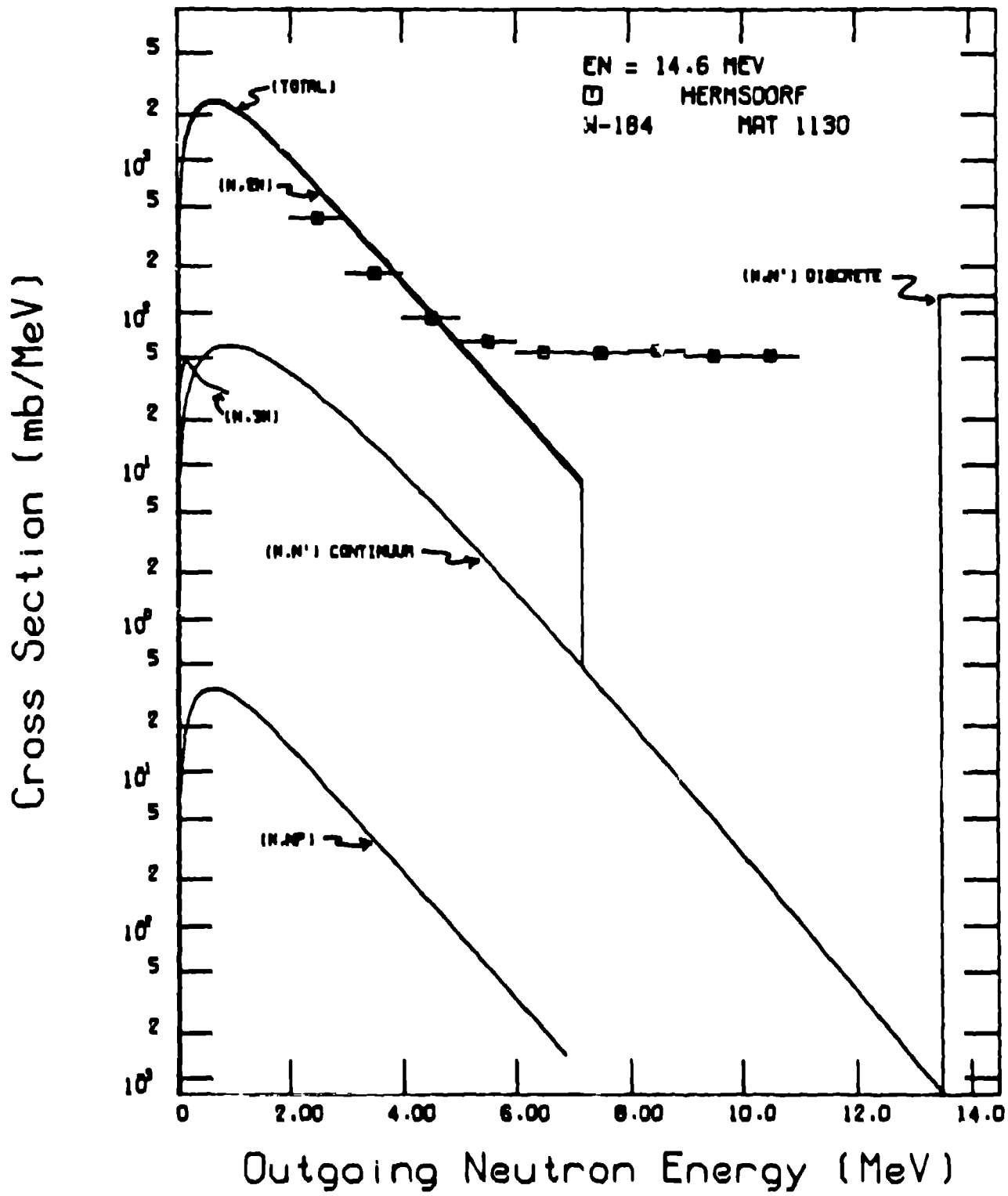
EN = 14.6 MEV
HERMSDORF
W-184 MAT 1130
(TOTAL)
(N,EN)
(N,N') DISCRETE
(N,N') CONTINUUM
(N,2N)
(N,NP)
Cross Section (mb/MeV)
Outgoing Neutron Energy (MeV)
0
2.00
4.00
6.00
8.00
10.0
12.0
14.0

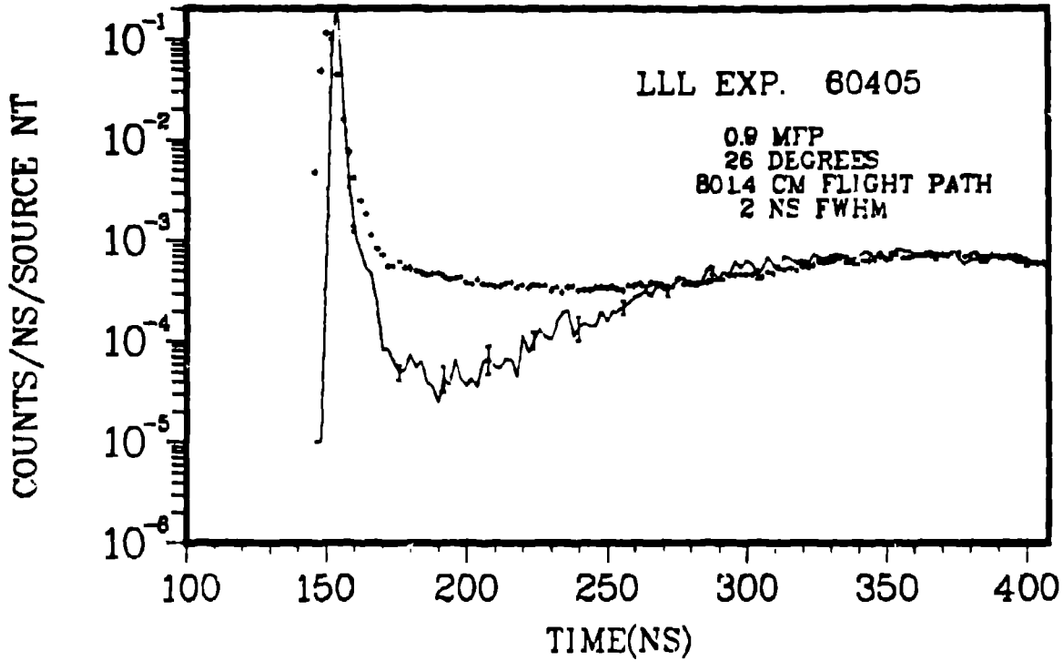
LLL EXP. 60405
0.9 MFP
26 DEGREES
8014 CM FLIGHT PATH
2 NS FWHM
COUNTS/NS/SOURCE NT
TIME(NS)

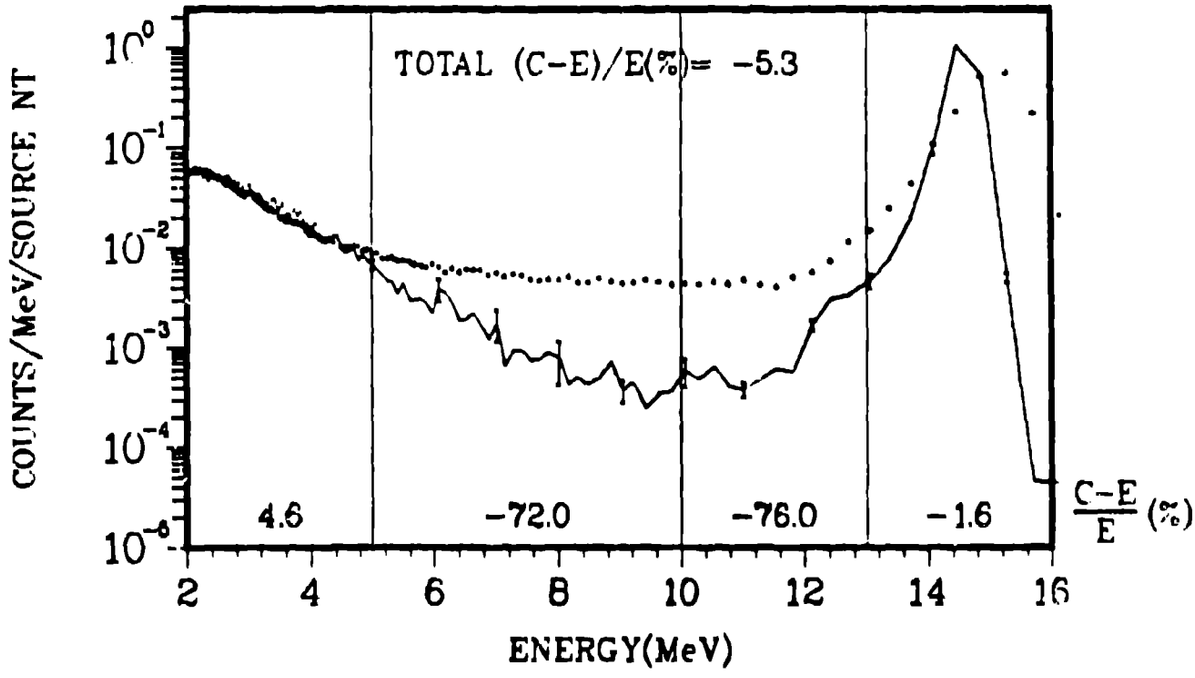
TOTAL (C-E)/E(%)= -5.3
4.6
-72.0
-76.0
-1.6
C-E/E (%)
COUNTS/MeV/SOURCE NT
ENERGY(MeV)

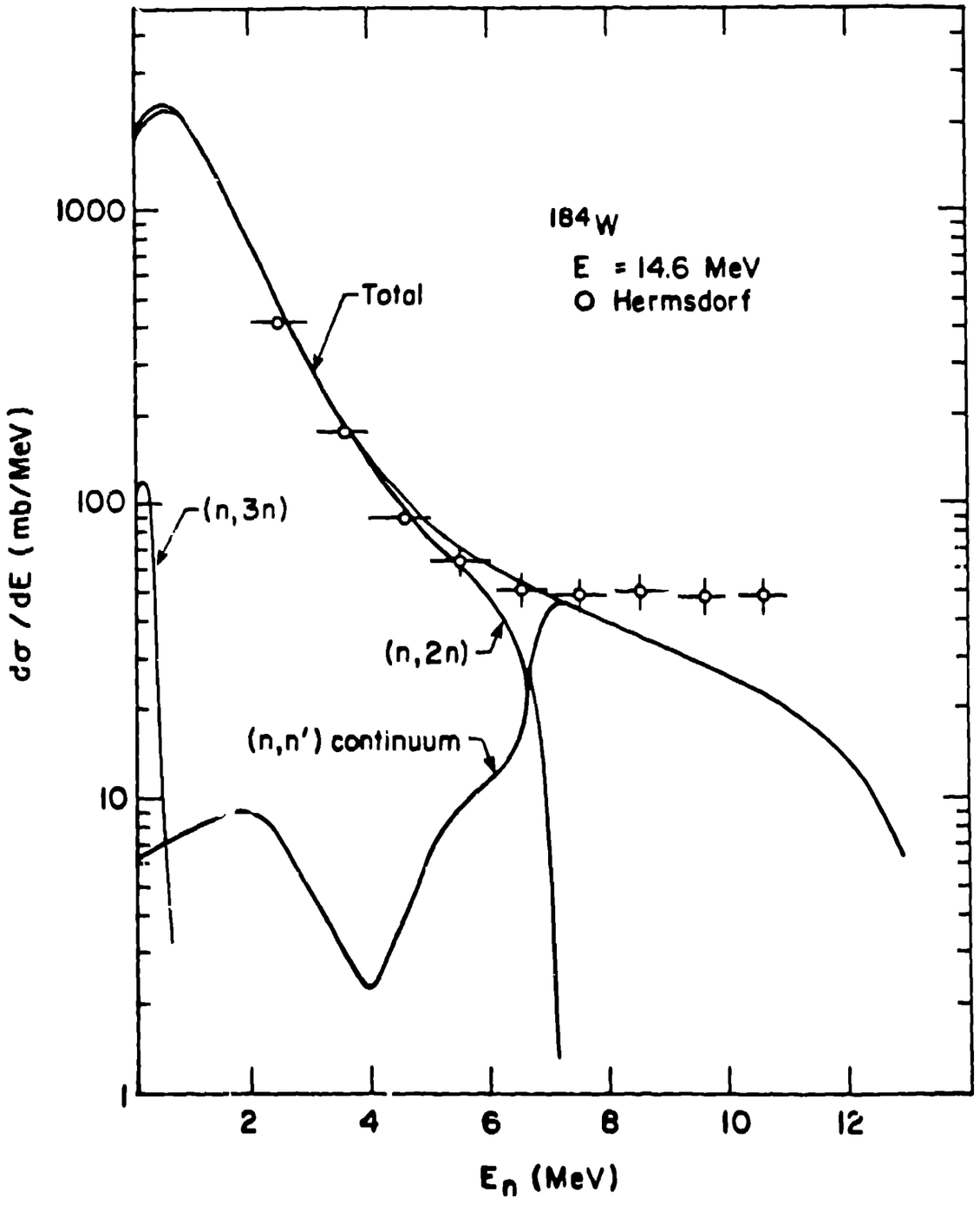
184W
E = 14.6 MeV
O Hermsdorf
Total
(n,3n)
(n,2n)
(n,n') continuum
1000
100
10
1
2
4
6
8
10
12
dσ/dE (mb/MeV)
En (MeV)

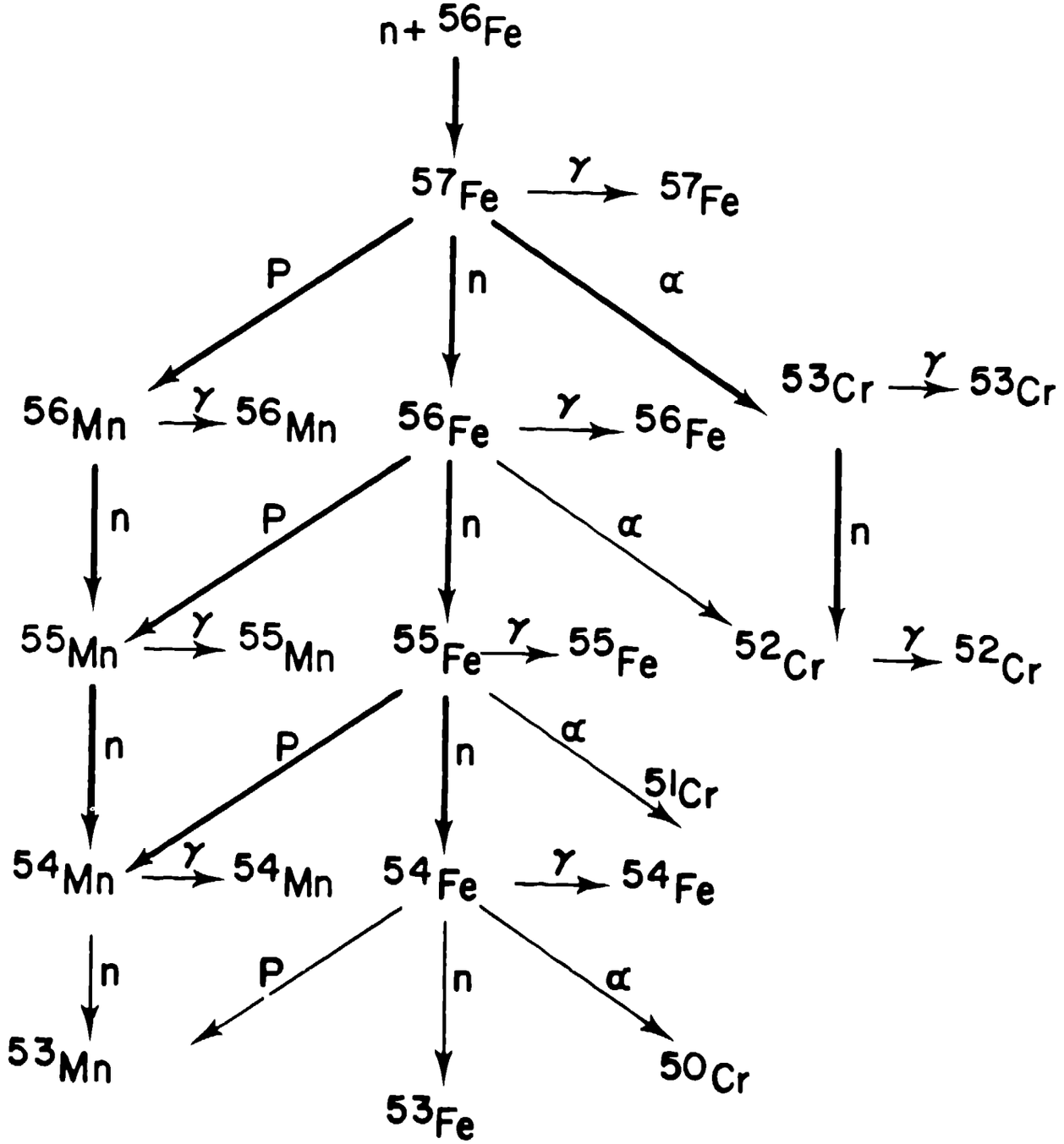
n+ 56Fe
57Fe
γ
57Fe
P
n
α
56Mn
γ
56Mn
56Fe
γ
56Fe
53Cr
γ
53Cr
n
P
n
α
n
55Mn
γ
55Mn
55Fe
γ
55Fe
52Cr
γ
52Cr
n
P
n
α
51Cr
54Mn
γ
54Mn
54Fe
γ
54Fe
n
P
n
α
53Mn
53Fe
50Cr

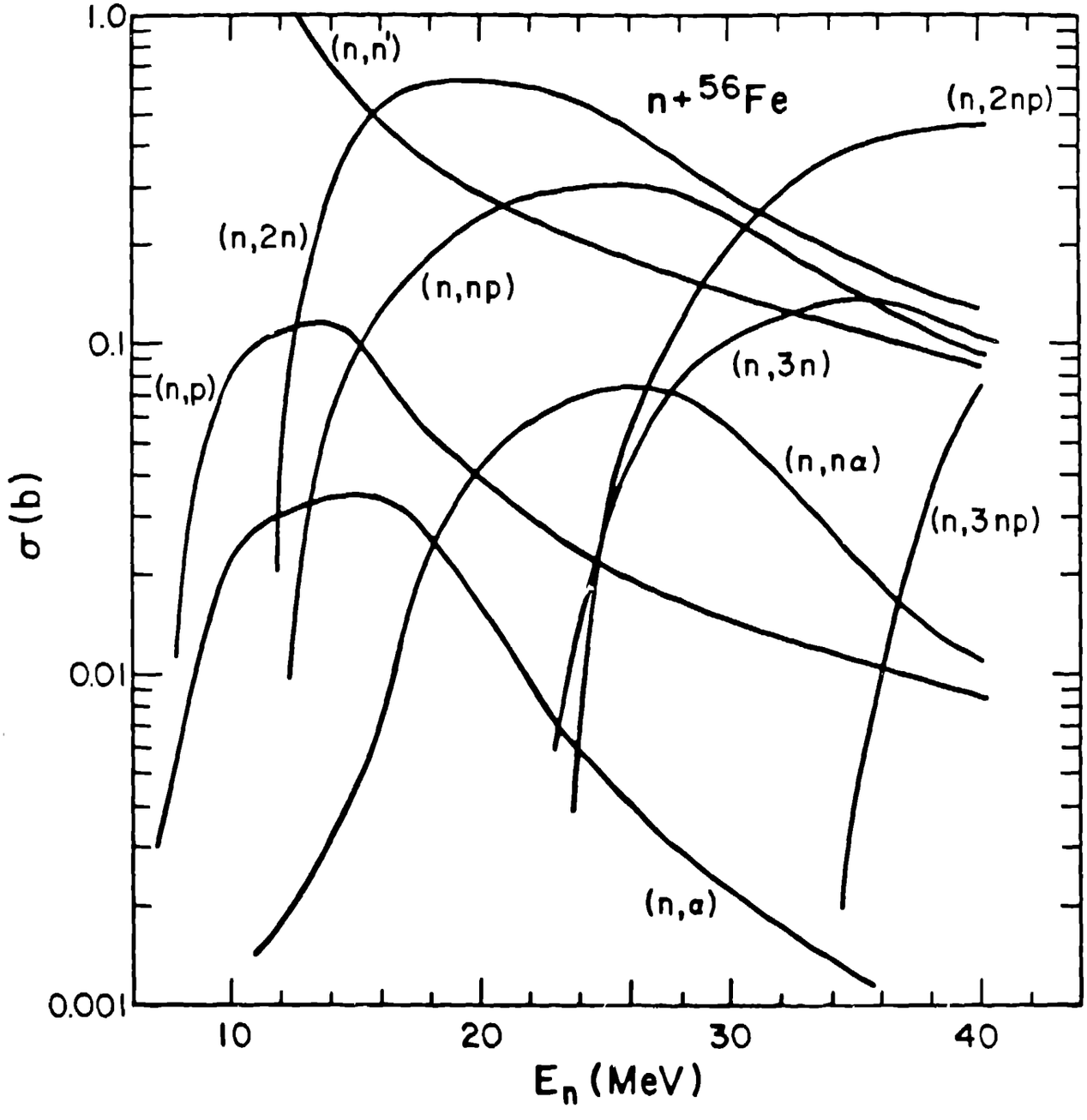
1.0
0.1
0.01
0.001
σ (b)
10
20
30
40
E_n (MeV)
$n+^{56}Fe$
(n,n')
(n,2n)
(n,np)
(n,p)
(n,3n)
(n,nα)
(n,3np)
(n,2np)
(n,α)

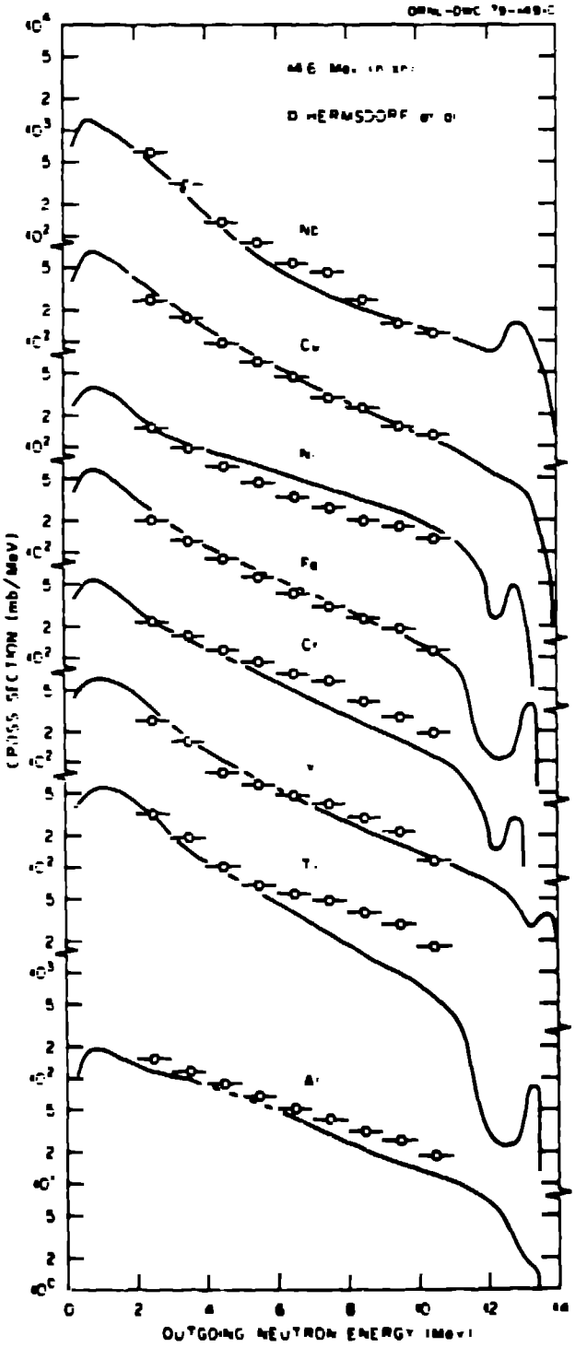
HERMSDORF
Ni
Fe
Cr
Ti
Ca
OUTGOING NEUTRON ENERGY (MeV)